Experimental Collapse of a Lightly Reinforced Concrete Frame Subjected to High Intensity Ground Motions

W.M. Ghannoum[1] and J.P. Moehle[2]

[1] *Assistant Professor, Dept. of Civil, Architectural, and Environmental Engineering, University of Texas at Austin, Austin, Texas, USA, Email: ghannoum@mail.utexas.edu*

[2] *Professor, Dept. of Civil and Environmental Engineering, University of California at Berkeley, Berkeley, California, USA - Director, Pacific Earthquake Engineering Research Center, Email: moehle@berkeley.edu*

ABSTRACT :

Post earthquake reconnaissance studies show that the primary cause of collapse in older non-seismically detailed reinforced concrete buildings is the loss of vertical-load-carrying capacity in building components leading to cascading vertical collapse. In cast-in-place beam-column frames, the most common cause of collapse is the failure of columns, beam-column joints, or both. Once axial failure occurs in one or more components, vertical loads arising from both gravity and inertial effects are transferred to adjacent framing components. The ability of the frame to continue to support vertical loads depends on both the capacity of the framing system to transfer these loads to adjacent components and the capacity of the adjacent components to support the additional load. When one of these conditions is deficient, progressive failure of the building can ensue. Presented here are the results of a series of dynamic tests performed on a one-third-scale, three-story, three-bay concrete frame. This large experiment was aimed at investigating the structural framing effects on local column failures and conversely the effects of localized column failures on the frame's global collapse vulnerability. The test frame was subjected to three high-intensity ground motion records before it suffered complete collapse. The gradual loss of column shear and axial load carrying capacities throughout the tests has given significant insight into the progressive collapse behavior of this type of frame.

KEYWORDS: Concrete, frame, column, collapse, dynamic, shear failure

1. INTRODUCTION

The broad objective of the presented experimental study is to investigate the seismic collapse behavior of non-seismically detailed reinforced concrete frames. Collapse is defined as the loss of axial load carrying capacity of one or more elements leading to partial or complete vertical subsiding of a structure. Particularly, the aim is to investigate structural framing effects on column shear and axial failures and conversely the effects of localized column failures on frame-system collapse vulnerability. As failure of one or more columns in a frame system does not necessarily constitute the collapse of that structure, understanding these interactions is essential in assessing the collapse vulnerability of this type of structure.

To date, there have been relatively few tests on lightly confined reinforced concrete frame systems in the literature (e.g., Bracci et al. (1992); Calvi et al. (2002); Otani and Sozen (1972); Shahrooz and Moehle (1987)) with even fewer conducted dynamically to collapse (Elwood (2002); Wu (2007)). In an attempt to fill some of this knowledge gap a 2-D, three-bay, three-story, third-scale reinforced concrete frame was dynamically tested to collapse. This frame contained non-seismically detailed columns whose proportions and reinforcement details allow them to yield in flexure prior to initiating shear strength degradation and ultimately reaching axial collapse. These columns are hereafter referred to as flexure-shear critical (FSC) columns. The interest in this class of column stems not only from their ability to withstand moderate to large deformations prior to axial collapse (Elwood and Moehle (2005); Sezen and Moehle (2006)) but from the fact that current codes of practice and design guidelines under-estimate their deformation capabilities, often leading to overly conservative predictions of structural collapse.

Experimental results are presented with focus on shear and axial degradation of the flexure-shear critical columns that lead to frame collapse. System level behavioral aspects are examined with particular attention given to load redistributions and dynamic amplifications that result from column failures.

2. EXPERIMENTAL PROGRAM

To study the collapse behavior of reinforced concrete frames with light transverse reinforcement, a three-bay, three-story frame was built and dynamically tested on the University of California, Berkeley shaking table (Figure 1a). Final dimensions and reinforcement details of this frame were influenced by the following main considerations: laboratory and shaking table limitations, replication of column details from previous column tests, analytical capabilities, target mode of failure, and cost. Target failure mode for the test frame was that of partial collapse that would enable examination of load redistributions during collapse.

a)

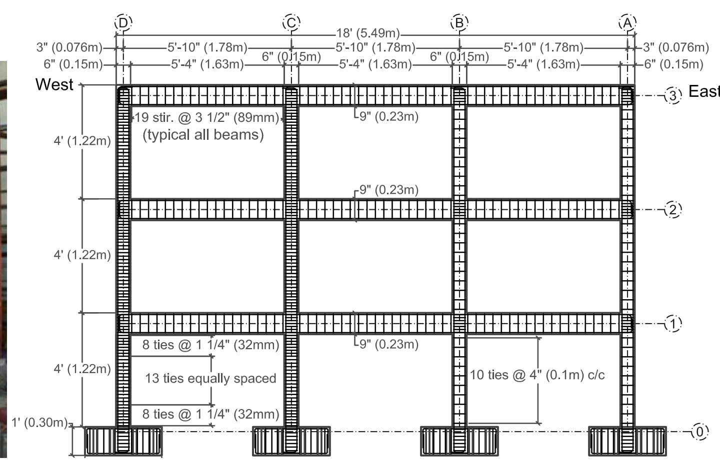

b)

Figure 1 Test frame photograph and details

These considerations resulted in the third-scale, two-dimensional reinforced concrete frame specimen shown in Figure 1 and detailed in Figure 1b. The frame was dimensioned to represent typical 1960s and 1970s office building construction in California. Two of the columns in this frame had identical non-seismic detailing with widely spaced ties closed with 90 degree hooks, while the other two columns had identical ductile detailing as per ACI 318-2005 (American Concrete Institute (ACI) Committee 318 (2005)) recommendations for special moment-resisting frames. As mentioned previously, the non-seismically detailed columns in this frame were dimensioned and reinforced such that they yield in flexure prior to developing shear or axial failure. Ties in these columns were spaced over the column height at 4 in. on centers. This resulted in a transverse reinforcement ratio $\rho''=0.0015$ ($\rho''=A_{st}/bs$, A_{st}=area of transverse reinforcement with spacing s, b=column width). Longitudinal steel ratio of these columns, defined as the cross-sectional area of longitudinal reinforcement divided by the gross section area, was $\rho_l=0.0245$. The two ductile columns had a maximum transverse reinforcement ratio $\rho''=0.011$ and a longitudinal reinforcement ratio $\rho_l=0.0109$.

Since typical reinforced concrete building frames contain columns with varying axial loads, dimensions, and reinforcing details, they sustain a staggered failure mechanism whereby different columns fail at different drifts. The ductile columns in the test frame, while not apparently representative of older existing construction, were introduced to simulate that effect. As well, these ductile columns were introduced to achieve the target partial collapse mechanism for the test frame. This arrangement was useful in studying load redistributions during structural collapse. Lastly, the final arrangement of ductile and flexure-shear critical columns shown in Figure 1b was chosen as it applied different loading and end-fixity conditions to the otherwise identically dimensioned and detailed FSC columns at column axes A and B.

Beam dimensions and longitudinal reinforcements were identical on all floors and spans. Beams were designed to support applied gravity loads while creating a strong-beam weak-column mechanism. Beams were chosen to be deeper (at 9 in. [0.23m]) than required to resist gravity loads so as to have ample torsional stiffness and strength to resist any accidental torsion that may be generated during strong shaking. This deeper beam profile also reduced joint shear stresses. Beam transverse reinforcements were designed to resist shear corresponding to the development of ultimate flexural strength.

Lap splice effects were not introduced in the frame as they were not within the scope of this study and joints were reinforced transversely to force failure in FSC columns. The planar test frame was cast in a horizontal position from a single batch of concrete, and subsequently lifted to the upright position. Test frame concrete cylinder compressive strength was $f'_c = 3.56$ ksi [24.6 MPa]. Longitudinal reinforcing steel had a measured yield stress of $f_y = 64.5$ ksi [445 MPa]. Beam and column ties were straightened basic bright wires with measured yield strengths of 81 and 95 ksi [558 and 655 MPa]. Evenly distributed lead-weights were attached to the beams with masses equivalent to those expected considering dead loads from a one-way slab system typical of office building construction. Lead-weights were clamped onto beams with contact points being one neoprene pad and one steel plate per packet. The flexible neoprene pads were used to reduce the stiffening effects of lead packets on beams. Lead-weights resulted in an axial load ratio of approximately $0.16A_g f'_c$ on the first-story center columns (A_g=column gross section area).

The test frame was subjected to the same ground motion record scaled to various amplitudes. The Llolleo station (component 100) ground motion record from the 1985 Chile earthquake at Valparaiso (Valparaiso 1985-03-03 22:47:07 UTC) was chosen for these tests. This motion was scaled up 4.06 or 5.8 times from its original acceleration amplitudes for the main dynamic tests. Table 2.1 summarizes the testing protocol. The ground motion time scale was divided by a factor of $3^{0.5}$ to satisfy similitude requirements.

Figure 2 plots the acceleration history of the scaled motion and the elastic response spectra for 5% critical damping (amplitude scale 4.06). For comparison purposes, this figure also superimposes the FEMA 356 (American Society of Civil Engineers (ASCE) (2000)) 2% in 50 years design spectrum at a site on the University of California, Berkeley campus less than 200 m [219 yd] from the Hayward fault, for soil class B. As can be seen from Figure 2, the test frame was able to sustain three high intensity ground motions before reaching collapse.

Table 2.1Test protocol

Test Description	Ground Motion	Amplitude Scaling Factor
Half-Yield Dynamic Test	Llolleo, Comp. 100	0.3625
Dynamic Test 1	Llolleo, Comp. 100	4.06
Dynamic Test 2	Llolleo, Comp. 100	4.06
Dynamic Test 3	Llolleo, Comp. 100	5.8

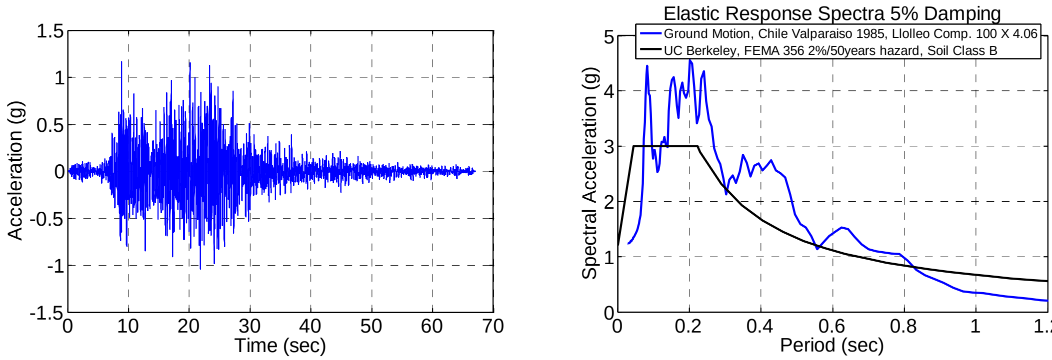

Figure 2 Input ground motion acceleration history and elastic response spectra (amplitude scaled by 4.06)

3. EXPERIMENTAL RESULTS

Based on Figure 1b, and for ease of reference throughout this document, columns will be referred to by their axis letter and story number.

3.1 Frame Global Behavior

During the Half-Yield Test, the frame sustained minor flexural cracking and softened slightly. During Test 1, the frame underwent large first-story horizontal drift ratios (-5.2%) and Column B1 sustained shear and axial failures at its base. Inter-story drift ratio is defined as the inter-story displacement divided by the clear story height (=39 in. [0.99m] for all frame stories). Figure 3a shows a picture of the base of Column B1 at the end of Test 1. Remarkably, even at this advanced damage state, Column B1 was still supporting approximately half its original axial load. The remaining axial load was shed to Columns A1 and C1, and generated uplift in Column D1. Even though Column A1 was identically dimensioned and detailed as Column B1 it did not sustain either shear or axial degradation in Test 1. Similarly Columns A2, A3, B2, and B3 did not show signs of shear failure either even though second story drifts ratios reached -4.7%. Shear and flexural cracks could be observed in test frame beams, with greater cracking severity observed in beams AB and BC at all floor levels. Also during this test, joints showed shear cracking and in some cases spalling.

During Test 2, Column B1 continued to degrade axially shedding more load to Columns A1 and C1 while its shear strength hovered around a residual capacity of approximately 1 kip [4.45 kN]. Column A1 meanwhile initiated shear failure and lost about two thirds of its shear capacity even though first-story horizontal drift ratios did not exceed 4%. Column A1 showed a very large shear crack at its base (Figure 3b) which resulted in slight shortening of the column (less than 0.1% vertical drift ratio = column vertical deformation/column clear height). No axial load capacity loss was reported in Column A1 during Test 2. Apart from damage to Columns A1 and B1, other frame members did not show any substantial change in their crack patterns during this test. Joints showed additional shear cracking and some spalling, particularly the first floor and edge joints.

(a) (b) (c)

Figure 3 (a) Column B1 at end of Test 1, (b) Column A1 at end of Test 2, (c) bare frame after collapse

During Test 3, Column A1 failed axially and collapsed the East side of the frame with it. Figure 3c shows a picture of the bare collapsed frame at the end of the testing program. Column C1 picked up a significant amount of axial load (about 12 kips [53.4 kN]) as Columns A1 and B1 collapsed vertically. Column D1 experienced a slight uplift. Both Columns A1 and B1 sustained relatively "gradual" axial collapses as they were able to hold a significant amount of axial load during the collapse. This resulted in a much slower collapse rate than free fall and translated into relatively low vertical acceleration amplifications.

3.2 Shear Failure of Flexure-Shear Critical Columns

3.2.1 Experimental Evidence

During dynamic testing, the identically dimensioned and detailed Columns A1 and B1 underwent almost matching inter-story drifts but initiated shear failures at different times due to differing loading and boundary conditions. Shear failure of Column B1 is initiated in Test 1 at a drift ratio of approximately -3.15% and a shear force of -9.9 kips [-44 kN] as identified by a square maker in Figure 4. Shear failure initiation is defined where shear strength loss commences and is associated with the development of a large shear crack. The diamond markers in Figure 4 identify the point at which the first shear cracks were recorded at the base of Columns A1 and B1. These cracks opened up to a maximum of about 0.02 in. [0.51 mm] in the deformation cycle in which they appeared but did not result in shear strength degradation at that time. In Column B1, shear strength degradation initiated a loading cycle after the formation of the first shear crack while in Column A1 no shear strength degradation was observed in Test 1.

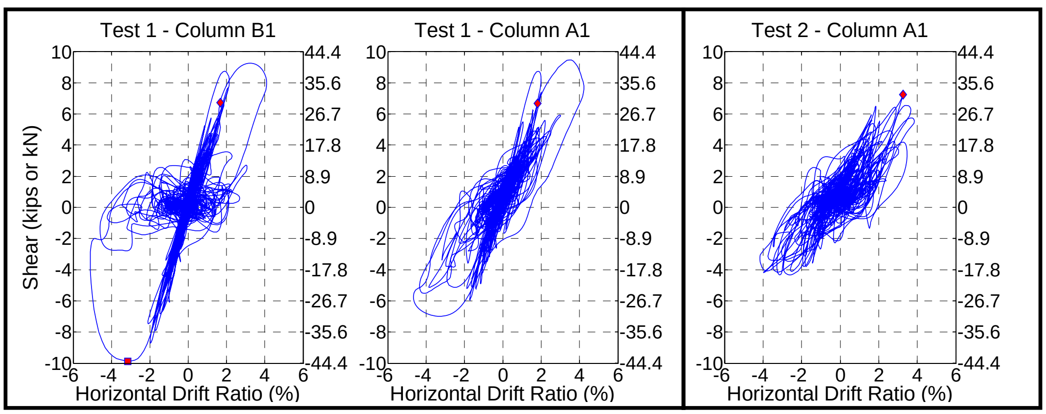

Figure 4 Columns A1 & B1 inter-story horizontal drift ratios versus shears – Tests 1 & 2

Shear failure at the bottom of Column A1 initiated during Test 2 at a horizontal drift ratio of approximately +3.26% and a shear force of 7.25 kips [32.2 kN] as identified by a square maker in Figure 4. Table 3.1 highlights differences in column response values at the initiation of shear failure of Columns A1 and B1. Table values include inter-story horizontal drift ratio, shear and axial forces, top and bottom moments, as well as top and bottom end region rotations. Table 3.1 also presents pertinent response values for Column A1 at axial failure initiation during Test 3.

Table 3.1 Column states at shear and axial failure initiation

Response Values	**Shear Failure Initiation**		**Axial Failure Initiation**
	Column B1 Test 1	**Column A1 Test 2**	**Column A1 Test 3**
Horizontal inter-story drift ratio, %	-3.15	3.26	1.61
Shear force, kips (kN)	-9.89(-43.9)	7.25(32.2)	2.91(12.9)
Axial force, kips (kN)	-24.7(-110.1)	-21.5(-95.5)	-16.3(-72.5)
Bottom moment, kip-in. (kN-m)	201(22.7)	-153(-17.3)	-38.1(-4.3)
Bottom end region rotation, rad	-0.0265	0.0259	N.A.*
Top moment, kip-in. (kN-m)	212(-23.9)	157(17.7)	84.2(9.5)
Top end region rotation, rad	0.0207	N.A.*	N.A.*

*: value not available as instruments were impacted during testing

At shear failure initiation during Test 2, Column A1 was under -21.5 kips [-95.5 kN] of axial load (compression), with shear force of 7.25 kips [32.2 kN], bottom moment of -153 kip-in. [-17.3 kN-m], and end rotation of 0.0259 rad. During Test 1, Column A1 was subjected to similar if not larger forces, drifts and end rotations than in Test 2; both in the positive and negative drift directions. This observation seems to indicate that the combinations of maximum deformations and loads applied to Column A1 were not sufficient in of themselves to initiate shear failure in that column. Rather, test results suggest that these maximum load-deformation combinations generated a shear crack in the column and subsequently weakened it through repeated cycling. Ultimately this may have lead to a sufficient reduction in shear capacity of Column A1 and initiated shear failure. Second story Columns A2 and B2 did not show signs of shear failure throughout testing even though second story inter-story drift ratios reached a maximum of -4.7% during Test 1.

3.2.2 Discussion

Both Columns A1 and B1 initiated shear failure at deformation levels well above yield; about 3 times yield to be more precise. These columns thus behaved as FSC columns. Imposed end-fixity boundary conditions were found to be of major importance in shear failure initiation of FSC columns. Assessing differing fixity boundary conditions was done through comparing column end rotations with inter-story horizontal drift ratios (Figure 5). End rotations were only monitored for the first and second story FSC columns of the frame (i.e. Columns A1, B1, A2, and B2). Figure 5 shows a clear difference between fixity conditions applied to first and second story columns. Figure 5 shows that for the same inter-story drift ratio, second story columns were under much smaller end rotations. This implies that joint rotations induced large rigid-body rotations in second story columns. These rotations combined with lower second-story axial loads could explain why second-story columns did not experience shear failures even though they were pushed to a maximum horizontal inter-story drift ratio of -4.7% in Test 1. Additionally, Figure 5 shows a large difference in end rotations for Columns A1 and B1 between top and bottom end regions. In this case as well, joint rotations were found to relieve end rotations at the tops of Columns A1 and B1. Shear failures occurred at the bottom of both Columns A1 and B1 where rotations were highest. Thus, experimental evidence indicates that column end rotations, rather than column drifts, may be better predictors of shear capacity reduction leading to shear failure initiation in FSC columns.

Furthermore, it was observed that a combination of framing-element flexural capacities and stiffnesses (e.g., Columns A1 and A2 framed into one beam while Columns B1 and B2 framed into two) and higher mode effects were major contributors to the observed high variability in end-fixity conditions. These factors are fairly common in RC frame structures indicating that this high variability in column boundary conditions is likely to be the norm rather than the exception in RC frame structures.

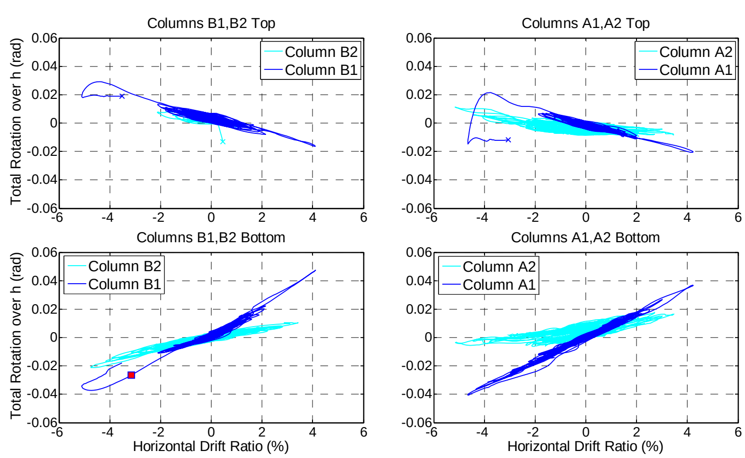

Figure 5 FSC column inter-story horizontal drift ratios vs. end rotations – Test 1

Axial load effects on shear failure initiation of FSC columns were highlighted by the axial load differences between Columns A1 and B1. Axial load in Column B1 was relatively constant throughout testing and always higher than that of Column A1. Column A1 underwent much larger axial load variations, which varied from slight tension in the negative drift direction to roughly the axial load level of Column B1 in the positive drift direction. The lighter axial loads in Column A1 also resulted in smaller moments and shear forces in that column, both in the elastic range due to tension softening and in the inelastic range due to the reduction in flexural yield strength associated with a reduction in compressive axial load. Thus with both Columns A1 and B1 experiencing similar levels of drifts and end rotations, the increased axial loads coupled with increased shear forces and moments in Column B1 appear to have been the determining factors in why Column B1 failed in shear prior to Column A1. It was not possible in these experiments to dissociate the effects of increased axial loads from their associated increased shear forces and bending moments.

Columns A1 and B1 sustained very different shear degradation mechanisms. While Column B1 appears to have lost most shear strength during a single cycle after shear failure initiation, Column A1 sustained multiple cycles past shear failure initiation at similar deformation levels and experienced shear strength degradation due to cycling (Figure 4). In other words, the shear versus drift relation of Column B1 traced a shear failure envelope whereas Column A1 sustained more of a low-cycle fatigue failure with shear capacity diminishing with each successive deformation cycle and accumulation of damage in the critical region. This implies that shear strength degradation in FSC should not only be defined using a backbone curve but should also include a damage related parameter that would reduce column shear capacity with deformation cycles beyond shear failure initiation.

3.3 Axial Failure of Flexure-Shear Critical Columns

3.3.1 Experimental Evidence

During Test 1, Column B1 experienced axial shortening and loss of axial load capacity. Remarkably, even at the advanced damage state observed at the end of Test 1 and after subsiding about 0.3 in. [7.6 mm] vertically, Column B1 was still supporting approximately half its original axial load. Column B1 axial load degradation occurred over a span of approximately 12 seconds in Test 1. Once degradation initiated, its duration roughly coincided with the duration of strong shaking. The rate at which axial shortening accumulates is thus likely linked to amplitude and amount of horizontal drift cycles. This behavior is indicative of low-cycle fatigue damage and axial-shear interaction. A linear relation between axial load and axial drift was observed throughout the shortening of Column B1. This relation can be attributed, at least partly, to the relatively constant stiffness of surrounding framing elements that relieve Column B1 of axial load. Initiation of shear failure in Column B1 was difficult to pinpoint due to its gradual nature and appeared to occur just after shear degradation is initiated in this column. This gradual axial failure produced only slight vertical acceleration amplifications at Joints B1 and B2. Column B1 continued to degrade axially during the strong shaking part of Test 2 as it shed most axial. The degrading relation between axial load and vertical drift continued the downward trend observed in Test 1 with slight softening observed in frame redistributing elements.

Column A1 collapsed axially due to the failure of its lower section in Test 3. The axial failure initiated at a horizontal drift ratio of +1.6% with an axial load of -16.3 kips [-72.5 kN]. Column shear before axial collapse hovered at less than 3 kips, a value reduced from column initial shear strength and attributed to damage incurred in the previous dynamic test. As Column A1 collapsed axially, the axial load it carried dropped to a low of about 10 kips [44.4 kN] initially and subsequently hovered between 10 and 15 kips [44.4 and 66.6 kN] until the frame collapse was halted by catching devices. Both Columns A1 and B1 sustained axial collapses were significantly slowed from free-fall as they were able to hold a significant amount of axial load during collapse.

3.3.2 Discussion

In Column A1, axial failure is observed to initiate only after shear strength is reduced to a fraction of its maximum value. For Column B1, axial failure initiation was difficult to pinpoint exactly but occurred roughly when shear strength was reduced to a residual value. Both these observations indicate that axial failure initiation occurs when shear strength is reduced substantially. The contrasting horizontal drift ratios at which axial failures initiate in Columns A1 and B1 (1.6% and about 4-5% respectively) indicate that drift may not be the driving force behind axial failure. Rather, a sufficient reduction in shear strength appears to be the driver, regardless whether that reduction occurred in one cycle (i.e., Column B1) or through fatigue (i.e., Column A1).

The effects of framing on column axial degradation were clearly demonstrated through the contrasting failures of Columns A1 and B1. In the case of Column B1, frame elements were able to redistribute axial load in excess of column capacity. This resulted in a gradual axial failure, which seemed to relate to the stiffness of the relieving framing elements and the amplitude of lateral deformations imposed during axial failure. In the case of Column A1 where the frame could not redistribute excess axial load, axial degradation occurred more rapidly and proceeded without pause until complete collapse. In this case however, the rate of collapse was slowed down significantly by the crushing of material in the failing region. These results thus provide approximate bounds on the rate of axial collapse of the specific FSC columns of the test frame. In both cases however, the rate of collapse was “relatively” slow and resulted in low dynamic amplification of vertical accelerations.

4. CONCLUSIONS

Frame geometry and layout of critical elements are crucial in determining failure sequence and ultimately collapse mechanisms. An edge column in a frame behaves much differently from an interior one. The differences are attributed to axial load variability, as well as stiffness and flexural capacity of framing elements.

Inter-story drifts do not correlate well with either shear or axial failure of FSC columns. Shear failure initiation appears to be deformation driven and is found to relate more to column end rotations than column drifts. Shear strength was observed to degrade both monotonically with increasing lateral deformations, as well as cyclically due to accumulation of damage with lateral deformation cycles. Axial failure was observed to initiate when shear damage reduces shear capacity significantly to almost residual. Consequently, axial failure initiation was not found to relate to deformations.

Compressive axial loads and associated yield moments and shear forces are negatively correlated with deformation capacity of FSC columns at shear failure initiation. It was not possible to isolate the influence of axial load from the associated peak lateral loads in the experiments.

Axial collapse behavior of FSC columns is governed by adjacent framing elements and their ability to redistribute axial loads. Stiffer framing elements produce a more gradual axial subsiding mechanism that is governed by number and amplitude of lateral deformation cycles. The absence of relieving frame elements produces an axial collapse mechanism that, once initiated, continues up to complete collapse. In this latter case, the rate of vertical subsiding is slowed down substantially by crushing of material in the failing region. In both cases the rate of vertical subsiding did not produce substantial vertical acceleration amplifications.

5. ACKNOWLEDGEMENTS

This work was supported by the Pacific Earthquake Engineering Research Center through the Earthquake Engineering Research Centers Program of the National Science Foundation under award number EEC-9701568. Any opinions, findings, and conclusions or recommendations expressed are those of the authors and do not necessarily reflect those of the National Science Foundation.

6. REFERENCES

American Concrete Institute (ACI) Committee 318. (2005). "Building Code Requirements for Reinforced Concrete (318-05)." American Concrete Institute, Farmington Hills, MI

American Society of Civil Engineers (ASCE). (2000). "Prestandard and Commentary on the Seismic Rehabilitation of Buildings." *FEMA 356*, Federal Emergency Management Agency, Washington DC

Bracci, J. M., Reinhorn, A. M., and Mander, J. B. (1992). "Seismic Resistance of Reinforced Concrete Strucutres Designed Only for Gravity Loads: Part III - Experimental Performance and Analytical Study of a Structural Model." *NCEER-92-0029*, State University of New York at Buffalo, Buffalo, New York

Calvi, G. M., Magenes, G., and Pampanin, S. (2002). "Experimental Test on a Three Storey RC Frame Designed for Gravity Only." *Proceedings of the Twelfth European Conference on Earthquake Engineering*, London, UK

Elwood, K. J. (2002). "Shake Table Tests and Analytical Studies on the Gravity Load Collapse of Reinforced Concrete Frames," PhD Dissertation, University of California, Berkeley

Elwood, K. J., and Moehle, J. P. (2005). "Axial Capacity Model for Shear-Damaged Columns." *ACI Structural Journal*, **102(4)**, 578-587

Otani, S., and Sozen, M. A. (1972). "Behavior of Multistory Reinforced Concrete Frames during Earthquakes." *Structural Research Series No. 392*, University of Illinois, Urbana-Champaign

Sezen, H., and Moehle, J. P. (2006). "Seismic Tests of Concrete Columns with Light Transverse Reinforcement." *ACI Structural Journal*, **103(6)**, 842-849

Shahrooz, B. M., and Moehle, J. P. (1987). "Experimental Study of Seismic Response of R.C. Setback Buildings." *87/16*, UCB/EERC, University of California, Berkeley

Wu, C.-l. (2007). "Gravity Load Collapse Experiments of RC Building Frames and Numerical Simulation." National Center for Research on Earthquake Engineering, Taipei